# Role of graphite oxide (GO) and polyaniline (PANI) in NO2 reduction on GO−PANI composites

**ARTICLE** *in* INDUSTRIAL & ENGINEERING CHEMISTRY RESEARCH · OCTOBER 2007

Impact Factor: 2.59 · DOI: 10.1021/ie070458a



**3 AUTHORS:**

Mykola Seredych
City College of New York
**112** PUBLICATIONS **2,704** CITATIONS
SEE PROFILE

Robert Pietrzak
Adam Mickiewicz University
**99** PUBLICATIONS **1,239** CITATIONS
SEE PROFILE

Teresa J Bandosz
City College of New York
**381** PUBLICATIONS **10,704** CITATIONS
SEE PROFILE

# Role of Graphite Oxide (GO) and Polyaniline (PANI) in $NO_2$ Reduction on GO-PANI Composites

**Mykola Seredych,[†] Robert Pietrzak,[†,‡] and Teresa J. Bandosz*[,†]**

*Department of Chemistry, The City College of New York, 138th Street and Convent Avenue, New York, New York 10031, and Laboratory of Coal Chemistry and Technology, Faculty of Chemistry, Adam Mickiewicz University, Grunwaldzka 6, 60-780 Poznań, Poland*

Graphite oxide−polyaniline (GO-PANI) composites were obtained by mixing graphite oxide with a polyaniline salt. The extent of surface reduction of the GO and polyanline (emeraldine) was increased by calcination at 350 °C. The surface characterization was done using Fourier transform infrared (FTIR) spectroscopy, X-ray diffraction (XRD), scanning electron microscopy (SEM), thermal analysis, potentiometric titration, elemental analysis, and adsorption of nitrogen at its boiling point. The materials were exposed to $NO_2$ to evaluate their activity for $NO_2$ retention/reduction on the surface. On all samples with the reduced form of polyaniline (emeraldine), a high efficiency for $NO_2$ reduction was observed. This efficiency was governed by the presence of PANI. Moreover, the presence of *N*-methylformamide solvent in the composite was determined to be an increasing factor for NO retention on the surface via its hydrogen bonding to the solvent that is interacting with the surface functional groups of graphite oxide. The calcination of GO-PANI at 350 °C reduced the GO surface, resulting in a physical mixture of graphite particles and reduced polyaniline (emeraldine). This happened because of the low thermal stability of compounds formed via the reactions of emeraldine with epoxy and carboxylic groups.

## Introduction

Growing concerns about the environment and concern regarding terrorist attacks have resulted in a search for effective adsorbents for the removal of small-molecule toxic gases (nitric oxides ($NO_x$), ammonia ($NH_3$), hydrogen sulfide ($H_2S$), sulfur dioxide ($SO_2$), carbon monoxide (CO), etc.). Because, usually, those gases are to be removed under ambient conditions in the presence of moisture, their physical adsorption is limited, because of weak adsorption forces. For these reasons, reactive adsorption, which is a variation of the adsorption process, must be explored.

One group of materials that have potential applications for the removal of small-molecules gases is based on graphite oxide (GO).[1−7] GO was first obtained in the 1850s, via the oxidation of graphite with such oxidants as $KClO_3/HNO_3$.[1] It has a layered structure and various nonstoichiometric chemical compositions, which are dependent on the level of oxidation. Extensive oxidation of graphite may lead to total molecular dissolution of graphite with carboxylic acids and $CO_2$ as the reaction products. As a result of the various levels of oxidation, the graphene layers of GO lose their polyaromatic character, because of the incorporation of various oxygen-containing functional groups.[2] Although the exact assignment of groups is controversial to some extent,[2−9] it is generally accepted that the graphene layers have epoxy and −OH groups that are attached to carbons.[2,3,5] According to Lerf and co-workers, the graphene layers are considered to be flat, with a slightly distorted tetrahedral configuration of carbons attached to −OH groups.[3] It was also proposed that the carboxylic groups are located at the edges of the graphene layers;[2] they have a strong acidic character.[2,4]

The graphene layers of GO are arranged in an organized way, with the interlayer distance ($d_{001}$) varying in the range of 6−12 Å. The main reason for those variations is in the level of hydration. Because epoxy and −OH groups exist within the interlayer space, the water molecules are attracted there by hydrogen bonding.[5] Moreover, both functional groups and water molecules are in different types of motion, depending on the location of the water, which can be either embedded or distributed in interlayer voids.

The layered character of graphite oxide opened a new route for the synthesis of composite materials. This route is possible because of (i) the hydrophobic character of GO, (ii) its easy dispersion in water, and (iii) delamination in alkaline media or alcohols. Moreover, graphite layers can be easily restacked, and their degree of orientation is dependent on the drying method.

A very popular way of GO modification is the introduction of amines or conducting polymers within the interlayer space.[10−14] The main goal of this type of modification is the production of functional nanometer-scale structures, devices, and particularly cathode materials for lithium secondary batteries. The introduction of large organic ammonium ions resulted in the initial exfoliation of layered structures, which were reassembled after drying.[10] When primary aliphatic amines were introduced, nucleophilic substitution reaction with surface epoxy groups occurred.[11] A study of GO intercalated with aniline/*o*-anisidine co-polymer indicated hydrogen bonds between the −NH, ═N−, and $-OCH_3$ groups and oxygen functional groups of GO as the main mechanism of intercalation.[12] Materials obtained in this way have electrical conductivities that are 3 orders of magnitude greater than that of pure GO. Moreover, the electrochemical response of the new material was significantly stabilized, in comparison with GO. An interesting way of the composite preparation was the formation of co-assembly layers from a colloidal dispersion of GO−amine in alcohol and cetyltrimethyl ammonium-intercalated bentonite.[14]

The objective of this paper is to evaluate the role of polyaniline (PANI) and GO in GO-PANI composites in the

* To whom correspondence should be addressed. Tel.: (212)650-6017. Fax: (212)650-6107. E-mail address: tbandosz@ccny.cuny.edu.
[†] Department of Chemistry, The City College of New York.
[‡] Laboratory of Coal Chemistry and Technology, Faculty of Chemistry, Adam Mickiewicz University.

10.1021/ie070458a CCC: $37.00 
Published on Web 09/15/2007

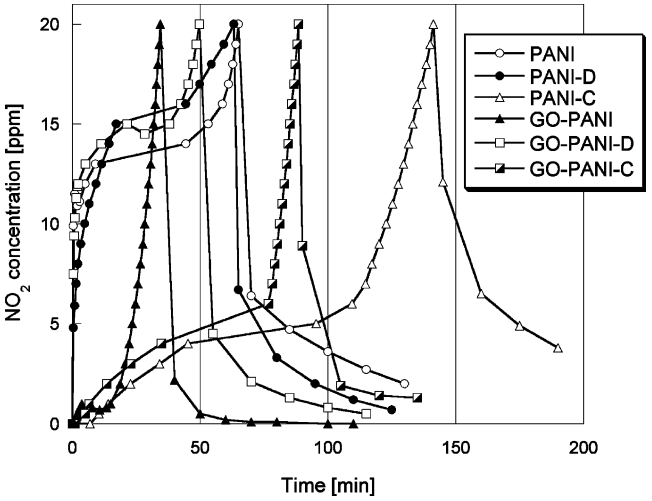


**Figure 1.** $NO_2$ breakthrough curves.

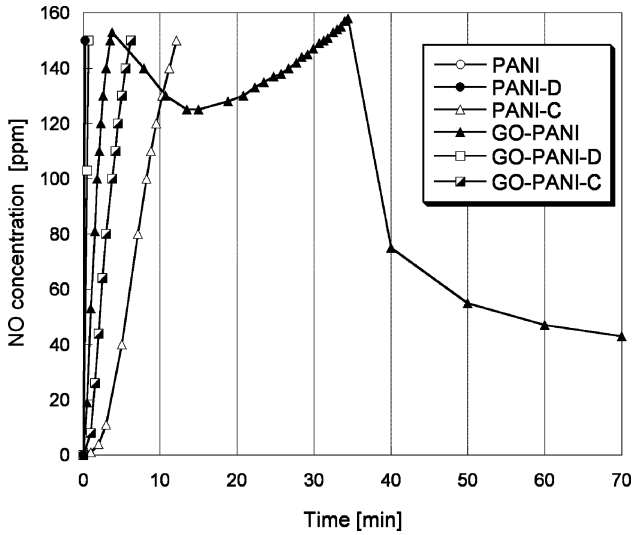


**Figure 2.** NO concentration curves.

process of $NO_2$ reduction/retention on the surface. The materials are modified by different levels of drying and heat treatment. These treatments are supposed to change the surface chemistry of graphite, as well as that of the composite, and also impose changes in the length and oxidation level of polyaniline monomers. They are expected to affect $NO_2$ retention on the surface and its reduction to nitrogen monoxide.

## Experimental Section

**(1) Materials.** The starting material, GO, was synthesized from graphite (average size of 38 $\mu$m) using the Hummers method.[15] Ten grams of graphite powder was stirred with 230 mL of cool (0 °C) concentrated sulfuric acid. Potassium permanganate (30 g) then was slowly added to the suspension. The rate of addition was controlled to prevent a rapid increase in the temperature of the suspension (should be <20 °C). The reaction mixture was cooled to 2 °C. After removal of the ice bath, the mixture was stirred at room temperature for 30 min. Distilled water (230 mL) was slowly added to the reaction vessel, to keep the temperature at <98 °C. The diluted suspension was maintained at 98 °C for 15 min and further diluted to 1.5 L with distilled water, followed by treatment with hydrogen peroxide (100 mL). The mixture was left overnight. The GO particles that settled at the bottom then were separated from the excess liquid by decantation. The remaining suspension

**Table 1. Carbon, Hydrogen, Nitrogen, Oxygen (and Chlorine) Content in Our Samples, and Chemical Formulas of the Materials Studied**

| | Composition [%] | | | | | |
|---|---|---|---|---|---|---|
| sample | C | H | N | O | Cl | formula |
| PANI | 77.7 | 4.0 | 15.1 | | 17.1 | $C_{6.5}H_{4.0}Cl_{0.5}N_{1.1}$ |
| PANI-D | 64.2 | 5.9 | 12.8 | | 3.2 | $C_{5.4}H_{5.9}Cl_{0.1}N_{0.9}$ |
| GO | 46.9 | 2.5 | <0.1 | 50.6 | | $C_{3.9}H_{2.5}O_{3.2}$ |
| GO-C | 80.7 | 0.1 | <0.1 | 19.2 | | $C_{6.7}H_{0.1}O_{1.2}$ |
| GO-PANI | 46.7 | 6.4 | 16.7 | 30.2 | | $C_{3.9}H_{6.4}O_{1.9}N_{1.2}$ |
| GO-PANI-D | 65.4 | 2.9 | 9.2 | 22.5 | | $C_{5.4}H_{2.9}O_{1.4}N_{0.7}$ |
| GO-PANI-C | 79.1 | 2.3 | 10.2 | 8.4 | | $C_{6.6}H_{2.3}O_{0.5}N_{0.7}$ |

**Table 2. Weight Loss during Heating in Nitrogen**

| | Weight Loss [%] | |
|---|---|---|
| sample | 30−120 °C | 30−350 °C |
| GO | 24.5 | 57.9 |
| GO-C | 0.6 | 1.2 |
| PANI | 12.5 | 31.3 |
| PANI-D | 1.9 | 23.1 |
| PANI-C | 0.5 | 0.9 |
| GO-PANI | 10.1 | 71 |
| GO-PANI-D | 1.9 | 24.3 |
| GO-PANI-C | 2.3 | 2.7 |

was transferred to dialysis tubes (the molecular weight (MW) cutoff was 6000−9000). Dialysis was performed until no $BaSO_4$ precipitate was detected during the addition of an aqueous solution of $BaCl_2$. The wet form of graphite oxide then was obtained by centrifugation. The gel-like material was freeze-dried, and a fine brown powder of the initial graphite oxide was obtained.

The sample was calcined in nitrogen at 350 °C for 3 h (GO-C), to impose exfoliation and control the surface chemistry.

PANI was used to modify the GO surface.[20] To obtain PANI, aniline was dissolved in 1 M HCl and cooled to 0 °C. Ammonium peroxydisulfate (1.15 equiv) then was added to the monomer solutions. The mixture was stirred at ice temperature for 1.5 h. The reaction mixture then was filtered and washed with 1 M HCl. The product of reaction was freeze-dried. Intercalation of polyanilines to graphite oxide was performed following the approach developed by Bourlinos and co-workers.[11] GO (1 g) was added to 110 mL of distilled water, and then the suspension was treated to sonication for 30 min. One gram of the PANI was added to 40 mL of *N*-methylformamide, and treated to sonication for 30 min. The polymer colloid that was prepared in this way was added to the GO suspension with sonification for 30 min. The mixture then was stirred overnight at room temperature. Several drops of concentrated HCl solution were added to the reaction mixture, which was stirred for another day, followed by heating at 60 °C for 1.5 h. The reaction mixture was then left overnight and centrifuged. Wet product was freeze-dried. The obtained material (GO-PANI) was heat-treated under nitrogen at 350 °C for 3 h, to impose changes in the surface functionalities (CO-PANI-C).

The GO-PANI sample was also dried at the oven at 120 °C and the material obtained in this way is called GO-PANI-D. For the sake of comparison, pure PANI was dried (overnight) at 120 °C in air and calcined at 350 °C in nitrogen for 3 h. These samples are called PANI-D and PANI-C, respectively.

**(2) Methods. (A) $NO_2$ Breakthrough Dynamic Test.** The home-designed dynamic test was used to evaluate $NO_2$ adsorption from gas streams.[16] PANI, GO, and composites thereof were ground (1−2 mm particle size) and packed into a glass column (length 370 mm, internal diameter 9 mm, bed volume of ∼2 $cm^3$) and used as received. Dry air with 0.1% of $NO_2$ was passed through the column of adsorbent at 0.450 L/min for $NO_2$. The

**Scheme 1. Calcination of the Emeraldine Salt**

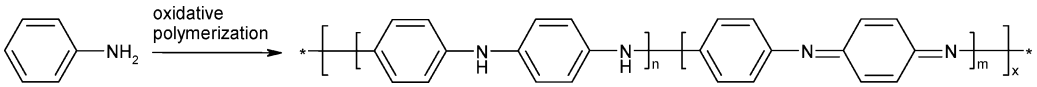


**Scheme 2. Possible Calcination of Emeraldine (Attached to the Surface Functional Groups) When Drying Is Applied**

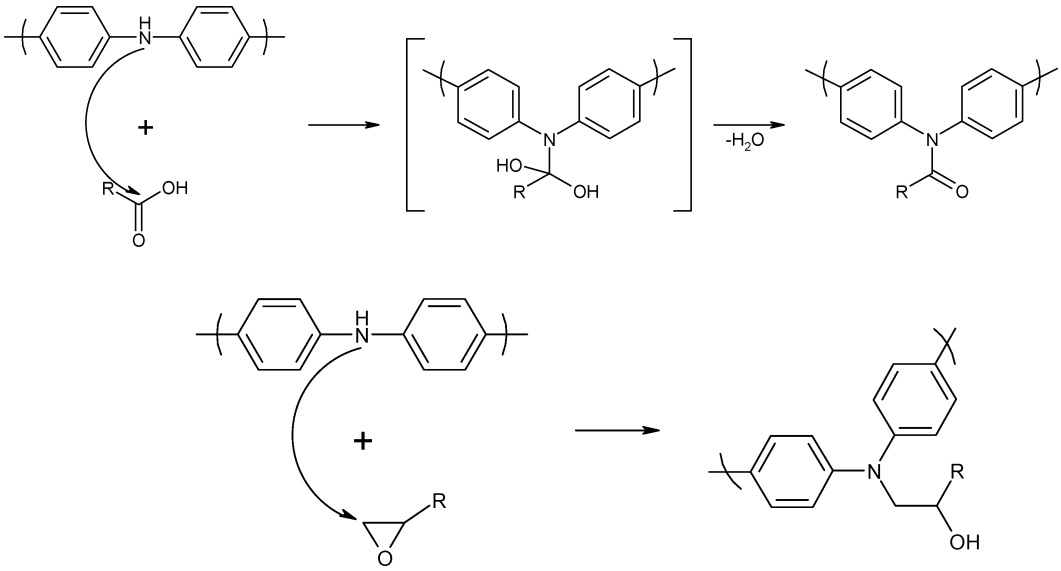


**Scheme 3. Reaction of Amino Groups at the End of the PANI Molecule with Carboxylic Acids To Form Emeraldine Salt**

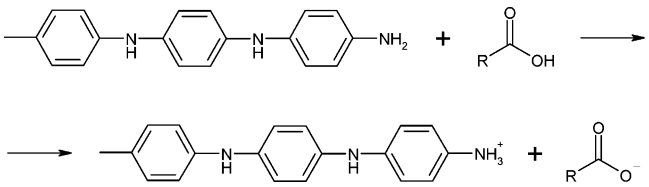


flow rate was controlled using Cole−Parmer flow meters. The breakthrough of $NO_2$ was monitored using electrochemical or photoionization sensors. The tests were stopped at the breakthrough concentration of 20 ppm. The interaction capacities of each sorbent, in terms of milligrams of toxic gases per gram of adsorbent, were calculated by integrating the area above the breakthrough curves, and from the $NO_2$ concentration in the inlet gas, flow rate, breakthrough time, and mass of sorbent. The breakthrough curves for $NO_2$ on GO adsorbents discussed in this paper are presented in Figure 1. To check the $NO_2$ reduction, the concentration of NO was also monitored up to 140 ppm (electrochemical sensor limit) (see Figure 2).

**(B) pH.** The pH of the initial samples and the exhausted samples after exposure to $NO_2$ was measured after an overnight stirring of a solution that contained 0.4 g of composite sample powder that was added to 20 mL of distilled water.

**(C) Thermal Analysis.** Thermogravimetry (TG) curves were obtained using a TA Instruments thermal analyzer. Approximately 30 mg of composite sample (initial and exhausted) was subjected to a regular increase of temperature at a heating rate of 10 °C/min, while the nitrogen flow rate was 100 mL/min.

**(D) X-ray Fluorescence (XRF) Analysis.** To determine the presence of chlorine, X-ray fluorescence (XRF) analyses were performed, using a Spectro 300 T system (ASOMA Instruments, Inc.) that was equipped with a Ti-target X-ray tube. The tube voltage was set at 24 kV with a current of 8 lA. The count and warm-up times were, respectively, 40 and 4 s. The region of interest (ROI) was between 7 keV and 11 keV, and a background correction was made between 12 keV and 17 keV.

**(E) Sorption of Nitrogen.** Nitrogen isotherms were measured at −196 °C, using an ASAP 2010 instrument (Micromeritics). Prior to each measurement, all samples were outgassed at 120 °C. Approximately 0.20−0.25 g of sample was used for these analyses. The surface area (via the Brunauer−Emmett−Teller (BET) method, $S_{BET}$), the microporous volume ($V_{mic}$, determined via the Dubinin−Radushkevitch (D-R) method),[17] the mesoporous volume ($V_{mes}$), and the total pore volume ($V_t$) were calculated from the isotherms.

**(F) X-ray Diffraction (XRD).** X-ray diffraction (XRD) measurements were conducted using standard powder diffraction procedures. Adsorbents were ground with methanol in a small agate mortar. The mixture was smear-mounted onto the zero-background quartz window of a Phillips specimen holder and allowed to air-dry. Samples were analyzed by Cu Kα radiation generated in a Phillips model XRG 300 X-ray diffractometer. A quartz standard slide was run to check for instrument wander and to obtain accurate locations of the $2\theta$ peaks.

**(G) Scanning Electron Microscopy (SEM).** Scanning electron microscopy (SEM) was performed on a model DSM 940 cold field emission instrument. The accelerating voltage was 2 kV. Scanning was performed in situ on a sample powder.

**(H) Fourier Transform Infrared (FTIR) Spectroscopy.** Fourier transform infrared (FTIR) spectroscopy was performed using a Nicolet model Magna-IR 830 spectrometer.

**(I) Potentiometric Titration.** Potentiometric titration measurements were performed with a DMS Titrino 716 automatic titrator (Metrohm). The instrument was set at the mode when the equilibrium pH was collected. Subsamples of the materials studied (∼0.100 g in 50 mL 0.01 M $NaNO_3$) were placed in a container that was thermostated at 298 K and allowed to equilibrate overnight with the electrolyte solution. To eliminate the influence of atmospheric $CO_2$, the suspension was continuously saturated with $N_2$. The carbon suspension was stirred throughout the measurements. Volumetric standard NaOH (0.1 M) was used as the titrant. The experiments were conducted in the pH range of 3−10. Each sample was titrated with base after the sample suspension was acidified.

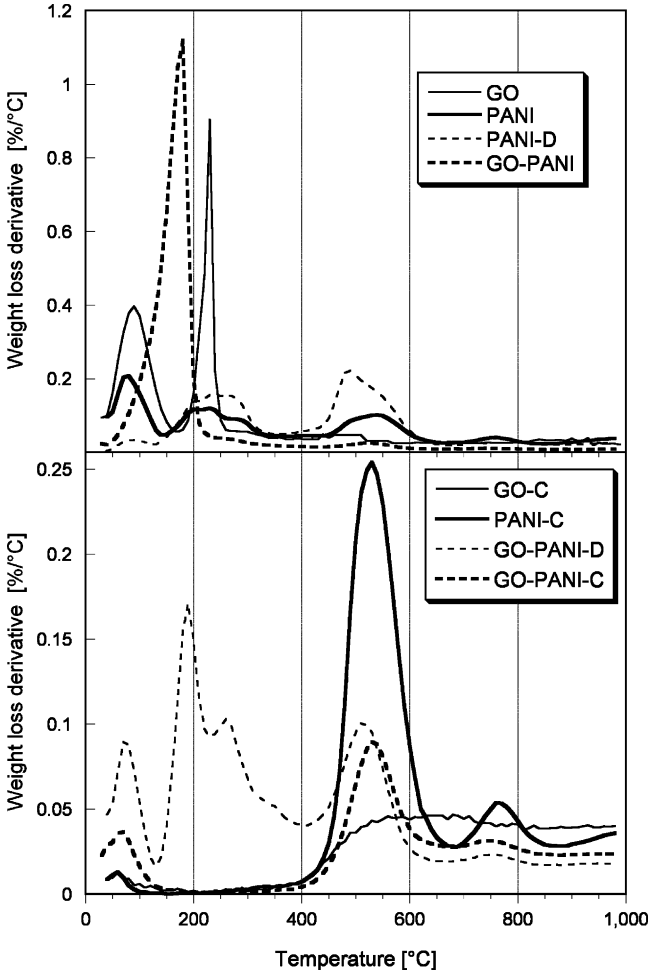


**Figure 3.** Differential thermogravimetry (DTG) curves in nitrogen for the composites obtained.

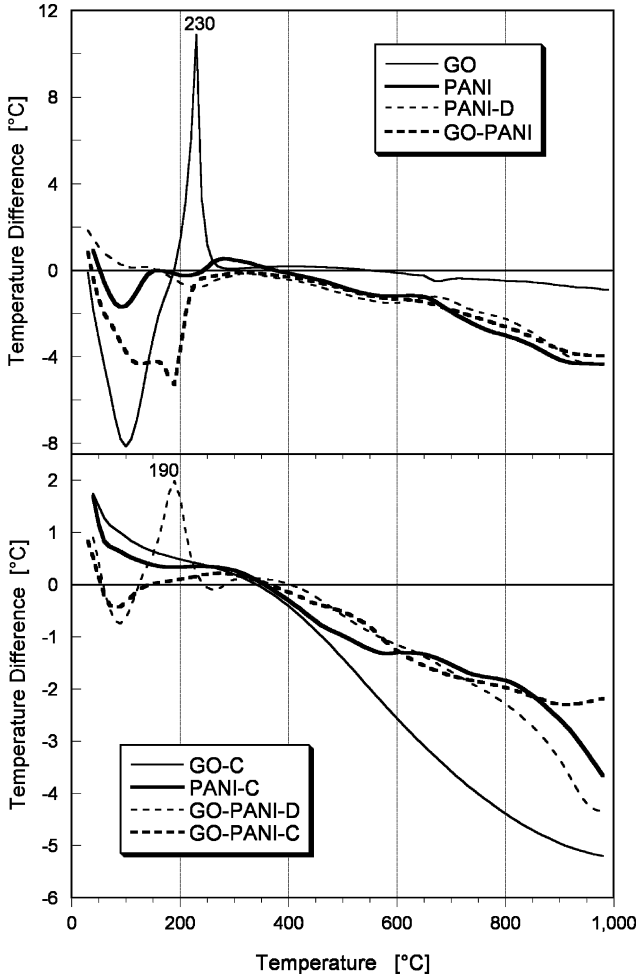


**Figure 4.** Differential thermal analysis (DTA) curves in nitrogen for the composites obtained.

The surface properties were evaluated first using potentiometric titration experiments.[18,19] Here, it is assumed that the population of sites can be described by a continuous p$K_a$ distribution, $f$(p$K_a$). The experimental data can be transformed into a proton binding isotherm, $Q$, representing the total amount of protonated sites, which is related to the p$K_a$ distribution by the following integral equation:

$$Q(\mathrm{pH}) = \int_{-\infty}^{\infty} q(\mathrm{pH},\mathrm{p}K_a) f(\mathrm{p}K_a)\, \mathrm{d}\mathrm{p}K_a \qquad (1)$$

The solution of this equation is obtained using the numerical procedure,[18,19] which applies regularization combined with nonnegativity constraints. Based on the spectrum of acidity constants and the history of the samples, the detailed surface chemistry was evaluated.

## Results and Discussion

The $NO_2$ breakthrough curves obtained on our materials are collected in Figure 1, along with the desorption curves. On pure GO and GO-C, the concentration of challenging gas reached a limit of 20 ppm immediately after the experiment began. Figure 2 presents the NO concentration curves. As observed, significant differences exist in the performance of materials. In all cases, $NO_2$ is almost immediately converted to NO, which is released from the system at high concentration exceeding the sensor limit. Only in the case of one sample, GO-PANI, did the concentration of NO stabilize, at ~140 ppm, relatively early in the experiment duration, when the detected $NO_2$ concentrations are small. It is interesting that, for this sample, the concentration of NO in the desorption run decreases with time to reach a plateau at 40 ppm. This plateau is likely related to NO that was strongly interacting with the surface of the adsorbent. These interactions are responsible for the slow kinetics of its release to the gas stream. On the other hand, the concentration on $NO_2$ in the desorption run for this sample decreases very fast to zero, which suggests either a lack of $NO_2$ in the system or its very strong retention on the surface. For all other materials, while the concentration of $NO_2$ decreases slowly in the desorption run, high concentrations of NO still are released, exceeding the maximum level readable by the sensor through the entire desorption runs. For the calcined materials, after a sharp decrease in $NO_2$ concentration at the beginning of the desorption runs, a few ppms of $NO_2$ still are released, which indicates its weak physical adsorption on the surface. That $NO_2$ is likely still converted to NO during the desorption run.

Drying the GO-PANI sample (such a sample is denoted as GO-PANI-D) has a dramatic effect on its performance. As a result of this process, high levels of $NO_2$ are detected immediately after the beginning of the test. The concentration of $NO_2$ stabilizes after reaching 15 ppm and became more or less constant for almost 50 min. The steep increase in the concentration then is noticed. This suggests lower efficiency of surface reaction than in the case of the freeze-dried sample. It is interesting that a similar behavior is observed for pure polyaniline; however, its surface is able to maintain levels of 15 ppm for an additional 20 min. Thus, the addition of GO has a negative effect on the performance of the composite in the process of

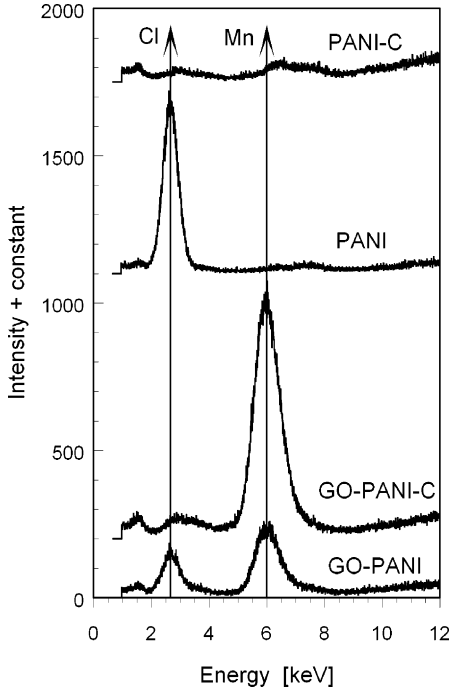


**Figure 5.** X-ray fluorescence (XRF) spectra for the GO-PANI, GO-PANI-C, PANI, and PANI-C samples.

$NO_2$ reduction. Calcination of GO-PANI and PANI results in a significant improvement of $NO_2$ concentration/retention on the surface. Although both materials exhibit a gradual increase in $NO_2$ concentration with time, the pure PANI-C once again seems to be the more-efficient medium for $NO_2$ conversion.

To understand the differences in the performance of our materials, the surface features must be analyzed. Table 1 presents the content of carbon, hydrogen, nitrogen, and oxygen (calculated) for our materials, along with the hypothetical formulas. The results indicate the significant content of chlorine in PANI. After the calcinations, the content of chlorine significantly decreases.

As a result of the oxidative polymerization of aniline, such as that used in our experimental procedure, emeraldine salt is expected to be formed in a partially oxidized form with the following formula:

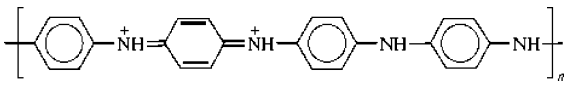

Calcination of this salt at 350 °C is expected to reduce the emeraldine salts further and increase the length of the monomers (see Scheme 1). As expected, the calcination of GO results in the removal of water and the decomposition of carboxylic groups located on the edges of the graphene layers.[20] Epoxy groups are considered to be still stable after heating at 350 °C. The incorporation of PANI to delaminated graphite oxide is expected to result in the formation of chemical bonds via nucleophilic substitution between the NH groups of emeraldine and the carboxylic and epoxy groups of GO.[11] The reaction schemes shown in Scheme 2 are possible when drying is applied. Moreover, amino groups at the end of the PANI molecule can react with carboxylic acids forming the salt (see Scheme 3). Although only a limited amount of PANI can undergo these reactions, because of the limited number of oxygen-containing groups on the GO surface and, thus, the significant amount of emeraldine is expected to be only in its reduced form, these chemical bonds can affect significantly the stability of the GO component surface.

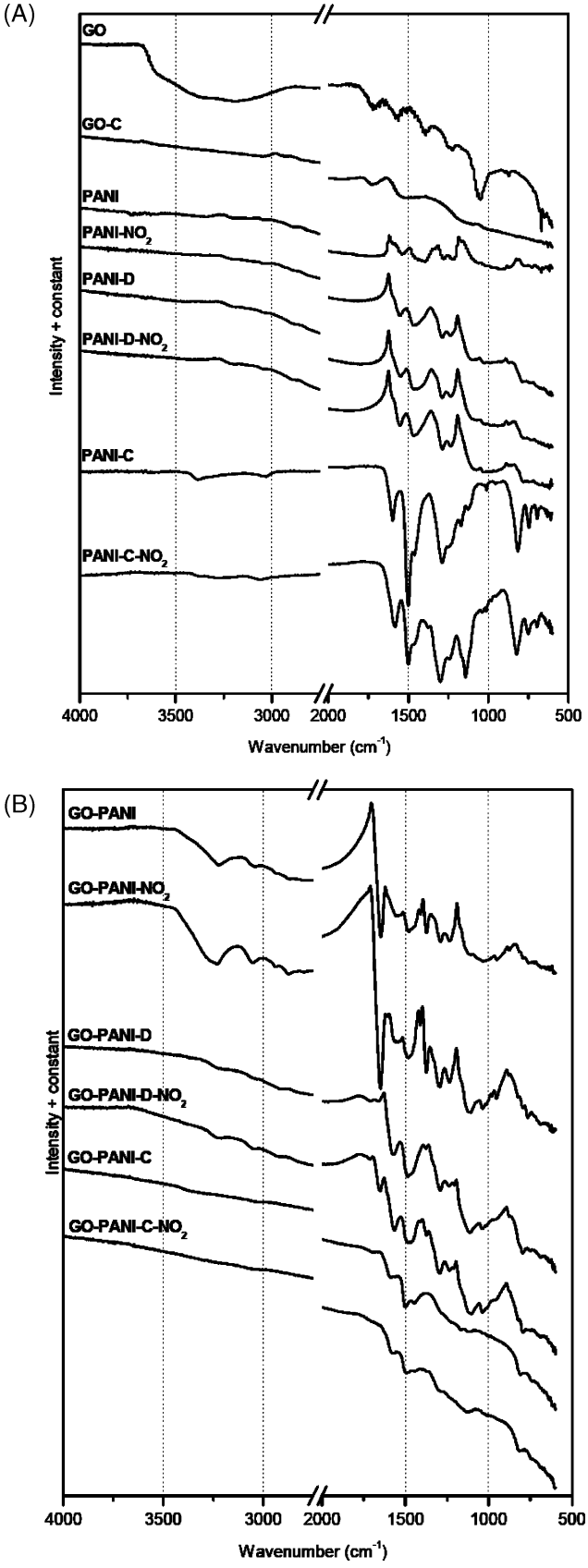


**Figure 6.** Fourier transform infrared (FTIR) spectroscopy curves for (A) the GO and PANI samples (initially and after exposure to $NO_2$) and (B) the GO-PANI composites (initially and after exposure to $NO_2$).

In fact, the chemical changes previously described can be seen in the formulas of our compounds derived from elemental

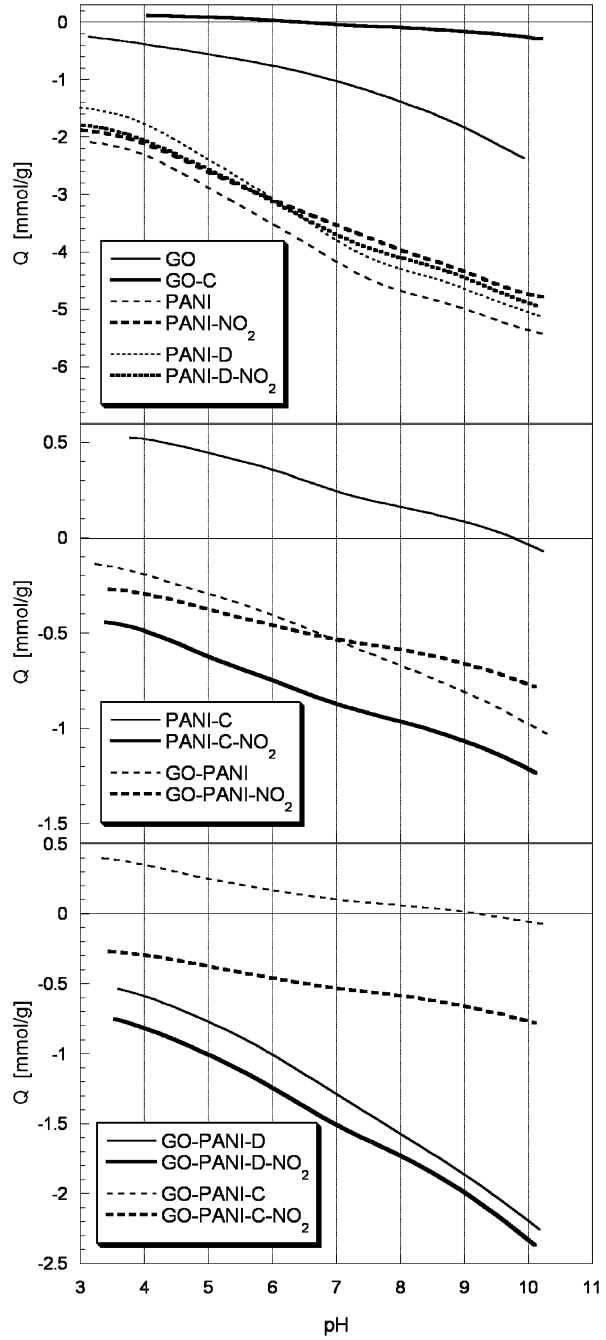


**Figure 7.** Proton uptake curves for the initial samples and after exposure to $NO_2$.

analyses (see Table 1). Although heating GO at 350 °C still leaves a significant amount of oxygen in the form of epoxy and −OH groups present between graphene layers,[20] in its mixture with PANI (the GO-PANI-C sample), much less oxygen is present in that sample than in the GO-C sample. Although the contribution of oxygen should decrease, because of the presence of nitrogen, that decrease is much more pronounced than in the case of the GO-PANI-C sample, when compared to the GO-C sample. For this sample, the amount of oxygen can be slightly overestimated, because it is calculated not taking into account chlorine, which should be still present in the composite.

An apparent discrepancy in our results is observed in the very high content of nitrogen in the GO-PANI sample (comparable to that in pure polyaniline). Taking into account the equal contributions of each component of the composite, the expected content of nitrogen in GO-PANI should be about half of that detected in PANI. We attribute that high nitrogen content to retention of *N*-methylformamide on the surface of the freeze-dried sample. Its small molecule can form hydrogen bonds with the epoxy groups on the surface. Supporting this belief is the fact that drying the material at 120 °C significantly decreases the nitrogen content in the sample.

Taking into account the weight loss of the samples when dried and calcined (Table 2), the content of PANI-C in the GO-PANI-C sample should reach 68%. This can explain the high content of nitrogen in this sample reaching 67% of its contents in PANI-C. Further analysis of the results presented in Table 2 confirms our hypothesis about the decomposition of surface functional groups upon calcination and the removal of the *N*-methylformamide that has been hydrogen-bonded to the surface. Even though, on the surface of the GO-PANI composite, much less water is retained, because of the introduction of an organic compound, which likely is partially replaced water located between the graphene layers of GO, and some water adsorption centers/functional groups are engaged in surface reactions with polyaniline, the huge difference between the weight loss at 350 °C and at 120 °C (60%) clearly indicates the removal of oxygen from epoxy groups that are involved in the formation of PANI/GO bonds and/or the removal of strongly bonded solvent that is intercalated between the graphene layers. When the GO-PANI composite is dried and then exposed to thermal analysis, only ∼20% of the sample mass is lost between 120 °C and 350 °C.

Detailed changes in the thermal decomposition of our compounds are observed in the differential thermogravimetry (DTG) curves that are presented in Figure 3, where the areas under peaks represent the extent of the weight loss at a certain temperature range. As seen from the graphs, there is a significant difference in thermal behavior between the GO-PANI composite and the separate GO and PANI samples. For all materials, the peak centered at ∼100 °C represents the removal of physically adsorbed water. This peak is visible as a small shoulder in a huge asymmetrical peak that is revealed between 30 °C and 200 °C, in the case of the GO-PANI composite, where the nonaqueous solvent was used. In the case of GO, the second peak between 200 °C and 250 °C represents the removal of carboxylic groups that are associated with the exfoliation of graphene layers, which is represented by exothermic peaks on a differential thermal analysis (DTA) curve (Figure 4).[12] The strong endothermic effect that is associated with that weight loss, in the case of the GO-PANI composite, with maxima noticed at 100 and 198 °C (Figure 4), can be linked to the evaporation water and an organic solvent (with a boiling point of 198 °C). On the other hand, for the dried GO-PANI sample (GO-PANI-D), the weight-loss pattern is much more complex than that for the GO-PANI composite. On the DTG curve of this sample, two peaks—with maxima at 180 and 225 °C—are present (see Figure 3). Because the first peak is associated with an exotherm on DTA cures (see Figure 4), it is related to the decomposition of surface functional groups, accompanied by some degree of exfoliation of the graphene layers.[12] This decomposition occurs at lower temperature than that in the case of pure GO. The second peak, which is linked to an exotherm, represents decomposition of the oxidized form of polyaniline (likely pernigraniline). There is a high probability that it is formed to some extent when the PANI is heated at 120 °C in air for an extended period of time. This compound is less thermally stable than emeraldine; therefore, more mass is lost during the heating of PANI than in the case of emeraldine (see

**Table 3. Surface pH Values and p$K_a$ and the Numbers of the Species Present on the Surface of the Materials Studied (Given in Parentheses)**

| sample | pH | p$K$ 3−4 | p$K$ 4−5 | p$K$ 5−6 | p$K$ 6−7 | p$K$ 7−8 | p$K$ 8−9 | p$K$ 9−10 | p$K$ 10−11 | all |
|---|---|---|---|---|---|---|---|---|---|---|
| GO | 3.12 | 3.05 (0.083) | 3.96 (0.225) | 5.23 (0.210) | 6.31 (0.228) | 7.23 (0.288) | 7.90 (0.280) | 8.96 (0.580) | 10.20 (0.811) | 2.705 |
| GO-C | 6.85 | | 4.91 (0.044) | | 6.18 (0.101) | 7.13 (0.062) | 8.62 (0.069) | 9.38 (0.065) | 10.33 (0.193) | 0.534 |
| PANI | 2.17 | 4.16 (0.416) | 4.68 (0.530) | 5.64 (0.617) | 6.65 (0.583) | 7.29 (0.593) | | 9.14 (0.491) | 10.03 (0.343) | 3.573 |
| PANI-$NO_2$ | 2.39 | 3.95 (0.373) | 4.79 (0.608) | 5.89 (0.491) | 6.84 (0.324) | 7.74 (0.521) | | 9.33 (0.721) | 10.29 (0.026) | 3.064 |
| PANI-D | 2.50 | | 4.29 (0.850) | 5.39 (0.694) | 6.41 (0.640) | 7.12 (0.723) | | 9.08 (0.594) | 10.11 (0.393) | 3.894 |
| PANI-D−$NO_2$ | 2.43 | | 4.04 (0.559) | 5.04 (0.577) | 6.13 (0.615) | 7.05 (0.592) | 8.10 (0.109) | 9.17 (0.633) | 10.24 (0.429) | 3.514 |
| PANI-C | 9.49 | | 4.73 (0.137) | | 6.41 (0.180) | 7.53 (0.068) | 8.73 (0.088) | | 10.15 (0.259) | 0.732 |
| PANI-C−$NO_2$ | 3.06 | | 4.33 (0.185) | 5.19 (0.108) | 6.42 (0.177) | 7.59 (0.080) | 8.77 (0.122) | | 10.08 (0.281) | 0.953 |
| GO-PANI | 3.40 | | 4.18 (0.169) | 5.64 (0.124) | 6.57 (0.121) | 7.35 (0.118) | 8.53 (0.175) | 9.96 (0.302) | | 1.009 |
| GO-PANI-$NO_2$ | 3.19 | | 4.20 (0.164) | 5.53 (0.066) | 6.31 (0.133) | 7.27 (0.050) | 8.09 (0.069) | 8.89 (0.156) | 10.19 (0.457) | 1.095 |
| GO-PANI-D | 3.02 | 3.80 (0.107) | 4.43 (0.146) | 5.21 (0.160) | 6.11 (0.287) | 7.08 (0.289) | 8.10 (0.279) | 9.14 (0.324) | 10.27 (0.511) | 2.103 |
| GO-PANI-D−$NO_2$ | 2.86 | 4.00 (0.208) | 4.99 (0.192) | 5.98 (0.276) | 6.86 (0.256) | | 8.03 (0.202) | 9.02 (0.315) | 10.17 (0.554) | 2.003 |
| GO-PANI-C | 8.26 | 4.03 (0.134) | 4.92 (0.089) | | 6.19 (0.101) | 7.24 (0.027) | 8.24 (0.046) | 9.68 (0.130) | | 0.527 |
| GO-PANI-C−$NO_2$ | 3.58 | | 4.28 (0.079) | 5.01 (0.098) | 6.38 (0.116) | 7.94 (0.055) | | 9.01 (0.096) | 10.17 (0.195) | 0.639 |

**Table 4. Structural Parameters Calculated from Adsorption of Nitrogen**

| sample | $S_{BET}$ [$m^2$/g] | $V_{mic}$ [$cm^3$/g] | $V_{meso}$ [$m^2$/g] | $V_t$ [$cm^3$/g] | $V_{mic}/V_t$ | $D_{BJH}$ [Å] |
|---|---|---|---|---|---|---|
| GO-PANI-$NO_2$ | 16 | 0.007 | 0.052 | 0.059 | 0.119 | 69 |
| GO-PANI-C | 20 | 0.009 | 0.060 | 0.069 | 0.130 | 73 |
| GO-PANI-C−$NO_2$ | 16 | 0.007 | 0.068 | 0.075 | 0.093 | 86 |

**Table 5. $NO_2$ Conversion Capacity and the pH Values of the Surface Before and After Exposure to $NO_2$**

| | $NO_2$ Breakthrough Capacity | | | pH | |
|---|---|---|---|---|---|
| sample | [mg/g of ads] | [mg/$cm^3$ of ads] | [mg/g of ads] at 5 ppm $NO_2$ | initial | exhausted |
| GO | 0 | 0 | 0 | 3.15 | |
| GO-C | 0 | 0 | 0 | 6.35 | |
| PANI | 10.40 | 2.9 | 0.33 | 1.63 | 1.70 |
| PANI-D | 8.80 | 2.5 | 0.25 | 1.75 | 1.74 |
| PANI-C | 83.15 | 23.3 | 64.29 | 9.85 | 2.24 |
| GO-PANI | 10.29 | 6.0 | 8.45 | 3.40 | 3.19 |
| GO-PANI-D | 7.92 | 3.0 | 0.24 | 3.02 | 2.86 |
| GO-PANI-C | 38.92 | 14.7 | 36.21 | 8.06 | 3.58 |

the DTG curve of PANI, in comparison with that for PANI-D). This is also consistent with the behavior of the GO-PANI-D sample in the process the $NO_2$ reduction discussed below. An absence of that exotherm in the case of GO-PANI suggests strong bonds of the solvent with the graphene layers, preventing exfoliation of the material. In regard to PANI, heating it to temperatures up to 350 °C in nitrogen apparently results in a mass loss of 31% (see Table 2), which can be linked to the release of HCl from the emeraldine salt (peak maximum at ∼230 °C) and chain scissions.[21,22] This should lead to a higher degree of surface reduction. In fact, the XRF spectra presented in Figure 5 shows a significant decrease in the content of chlorine in the GO-PANI-C sample, in comparison to that for the GO-PANI sample. The same pattern is noticed for the pure polymer.

The changes in the chemistry of our materials are also observed in the FTIR spectra presented in Figure 6. As observed, the spectra for the GO-PANI and GO-PANI-C samples represent the spectra of the corresponding composite materials.[4,23−28] The band at ∼1170 $cm^{-1}$ demonstrates the presence of a polyaniline salt (specifically emeraldine). The C−H in-plane bending deformation occurs at ∼1166 $cm^{-1}$ for the quinoid and ∼1172 $cm^{-1}$ for the benzoid ring.[23−28] Benzoid and quinoid vibrations are also detected as bands at ∼1500 and 1600 $cm^{-1}$. The absorption band at ∼1240 $cm^{-1}$, which is attributed to C−N stretching + ring deformation + C−H bending vibration modes,[27] is significant for the GO-PANI sample. It can be assigned to the $C-N^+$ stretching vibration in protonic acid-doped polyaniline. It indicates the formation on C−N coordinate-covalent bonds between the polymer chain and the carboxyl and epoxy groups onto the GO surface. After calcination at 350 °C, this band disappears. Carboxylic groups are observed on the GO surface as bands at 1120−1200 and 1665−1760 $cm^{-1}$, whereas the band at ∼1600 $cm^{-1}$ is attributed to the presence of epoxide groups.[23] O−H groups that are either attached to carbons or represent adsorbed water are detected as broad bands between 2200 and 3800 $cm^{-1}$.[23] A band at 3250 $cm^{-1}$, which represents the vibrations of −NH− groups of the *N*-methylformamide solvent, also is observed on the surface of the GO-PANI sample.[23] After drying, that band is much less pronounced and the band at 1410 $cm^{-1}$ disappears, which is linked to the change of the −C−N bonds that are associated with the benzoic ring into the −C−N bonds that are associated with the quinoid). Further heating has a more-pronounced effect on the surface chemistry of the GO-PANI-C sample. The bands that represent the −C−N coordinate-covalent bonds at 1233 $cm^{-1}$ and oxygen-containing groups are not present anymore, and the spectra resemble that of the PANI-C sample, with the quinoid and benzoic stretching vibrations detected at ∼1500 and 1600 $cm^{-1}$. Generally speaking, drying increases the contribution of quinoid structures, with their −C−N bonds being linked to the oxidized form of polyaniline, whereas calcinations increases the intensity of the bands that are related to benzoic structures.

The changes in acidity of our materials are revealed on the proton uptake curves presented in Figure 7. The most acidic of all the composite samples is the GO-PANI-D sample, and the most basic is the GO-PANI-C sample. The shapes of the curves indicate the heterogeneity of the surface functional groups. From the proton uptake curves, the distributions of acidity constants were calculated and the p$K_a$ values of the acidic species and the number of those species are collected in Table 3, along with the initial pH values of the suspensions used for titration. The larger number of acidic groups on the GO-PANI-D sample (twice that of the GO-PANI sample) can be explained by the presence of organic solvent between the graphene layers in the

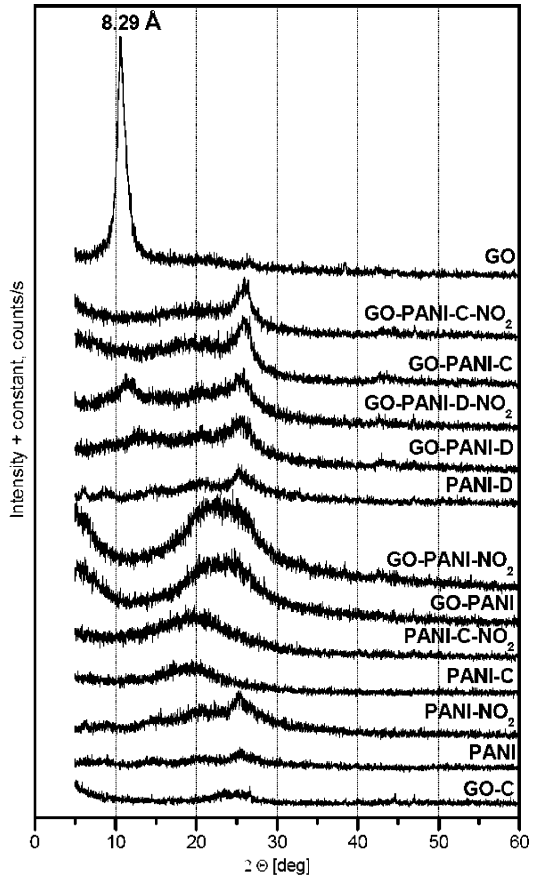


**Figure 8.** X-ray diffraction (XRD) spectra for the initial samples and the samples after exposure to $NO_2$.

case of the latter sample, blocking the access of the titrant to the surface functional groups. After removal of the *N*-methylformamide solvent, the oxygen-containing groups become more exposed and the acidity becomes similar to that detected in GO. Moreover, the polymer becomes partially oxidized. Calcination of composite at 350 °C significantly decreases the acidity, because the oxygen-containing groups decompose and only protons from the weak acidic nitrogen-containing groups of organic salt or −OH groups can be detected. Also, the calcination of PANI results in the predominantly basic materials, which supports the conclusion about the reduction of the emeraldine salt.

The GO well-organized layered structure can be noticed in its XRD spectra, which are presented in Figure 8, where the sharp peak at $2\theta$ represents 4.92 Å of interlayer space, where epoxy groups and water are present. After treatment with PANI, the disordered structure is detected,[29] which is demonstrated by a broad hub at $2\theta = 15°-35°$. After drying, the diffraction pattern of the GO-PANI-D sample resembles that of pure polyaniline, with broad peaks at $2\theta = 7°$, 14°, 20°, and 25°. On the other hand, for the PANI-C sample, only one broad hub is detected, which indicates the changes in the nature of the materials. Calcination of the GO-PANI composite results in a broad diffraction peak centered at $2\theta \approx 20°$ (the same as that for the PANI-C sample) and a relatively sharp peak at $2\theta \approx 25°$. The latter, even though it is present for PANI, likely represents the graphite layers, which are stacked together after the decomposition of surface functional groups. The GO-PANI-C composites, which are composed of physical mixtures of PANI-C and graphite, are shown in the SEM images presented in Figure 9, where, in addition to small particles of the latter, the heterogeneous granular aggregates of the PANI-C sample are observed. Those PANI aggregates, when formed in the composite, do not grow to the same extent as those in the PANI-C and PANI-D samples, where long tubular entities that are composed of polymer are observed.

Because the materials obtained were used as adsorbents of $NO_2$, the nitrogen adsorption isotherms were measured and the surface area and pore volume were calculated from them. The results collected in Table 4 show a practically nonporous structure. Although the GO-PANI composite is totally nonporous (not included in the table), drying of that material and its calcination at 350 °C results in the development of an area likely located between the stacked graphite particles and the agglomerates of PANI. The materials obtained can be considered as slightly mesoporous, with an average pore size of ∼70 Å.

The previously described differences in surface chemistry of the GO-PANI composites must affect the $NO_2$ retention/conversion on the surface. The $NO_2$ conversion capacities calculated from the breakthrough curve (Figure 1), along with the surface pH, are collected in Table 5. Based on the breakthrough measurements, the main process expected is the reduction of nitric dioxide to nitric oxide, according to the following reaction between emeraldine and $NO_2$, with pernigraniline (poly(1,4-iminoquinone-N-(1,4-phenilene)), NO, and water as the products:

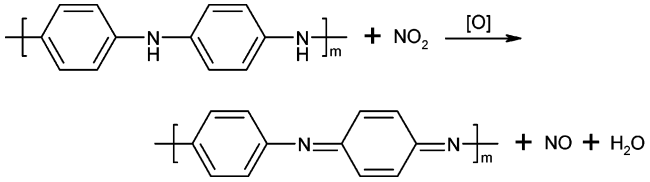


Moreover, when the PANI is attached to the surface functional groups, additional reactions can occur (as shown in Scheme 4).

A very interesting behavior toward the conversion of $NO_2$ and NO retention on the surface is observed for the GO-PANI sample. Only, in this case, the performance of the composite is better than that of PANI, which indicates the positive impact of the presence of GO on the overall properties of the material. The difference between this composite and other materials studied is the presence of *N*-methylformamide between the graphene layers. It is possible that the solvent molecules interact either with NO and $NO_2$ via polar and acid−base interactions (amide can be considered to be a weak base) and retain them, especially NO, which can explain the relatively low NO concentration during the desorption run. On the other hand, in the case of PANI, only the oxidation reaction of the reduced part of PANI can occur. After drying, the solvent is removed and, because GO is inactive in the process of $NO_2$ removal, only the PANI-D phase is responsible for the reduction of nitric dioxide to nitric oxide. When calcination is applied, changes in the emeraldine salt occur via an increase in the length of the polymers and in the contribution of its reduced form, which leads to more sites for oxidation and, thus, higher efficiency for $NO_2$ conversion. In fact, the conversion amount of $NO_2$ on the GO-PANI-C sample (see Table 5) is ∼47% of that on pure PANI-C, which clearly shows inactivity of the graphite phase. Moreover, from the rough evaluation of the contribution of each compound, given in Table 2, the GO has a negative effect on the capacity, likely because of its limiting influence on the growth of tubular entities. These entities might help in the retention of $NO_2$ on the surface.

Because elemental analysis of the sample, after exposure to $NO_2$, showed almost no changes in the level of nitrogen, only a trace amount of this gas can be retained on the surface; this

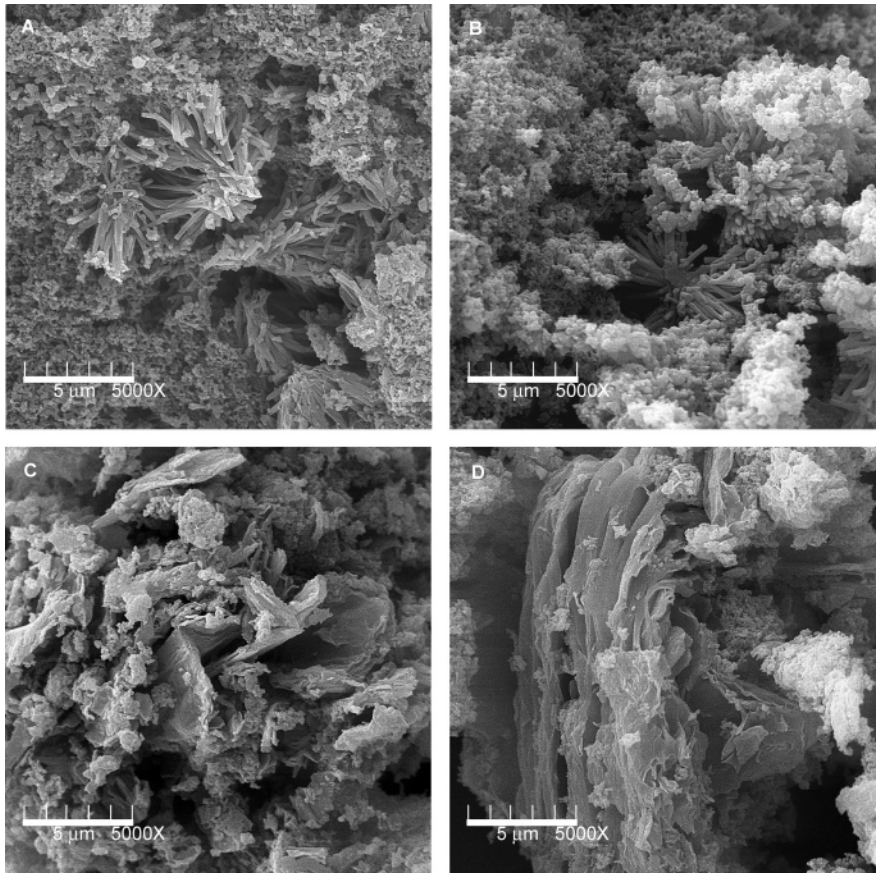


**Figure 9.** Scanning electron microscopy (SEM) images for (A) the PANI-C sample, (B) the PANI-D sample, (C) the GO-PANI-C sample, and (D) the GO-PANI-D sample.

**Scheme 4. Reactions That May Occur When PANI is Attached to the Surface Functional Groups**

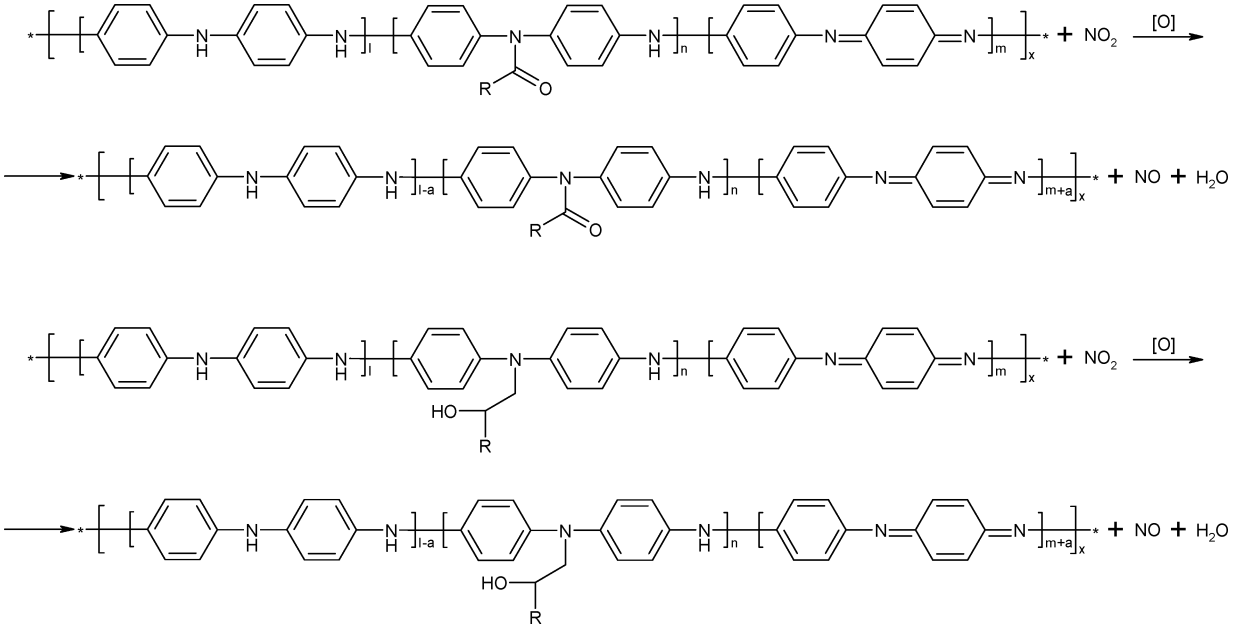


in agreement with the FTIR spectra, where no bands that represent $NO_2$/NO can be distinguished (see Figure 6). The main difference between the initial samples and those exposed to $NO_2$ is a decrease in the intensity of the band related to N−H vibrations at ∼1230 $cm^{-1}$ and an increase in the band that represents the streching N═Q═N ring (quinoid), at ∼1600 and ∼1170 $cm^{-1}$.[23−28]

The changes in surface chemistry are also observed in the pH values listed in Tables 3 and 5 and on proton uptake curves (see Figure 7). They clearly show an increase in the surface acidity after $NO_2$ exposure, caused by oxidation. The biggest increase in acidity is noticed for the GO-PANI-C sample after $NO_2$ adsorption. For this material, a new species with a p$K_a$ value of ∼5 are formed. It is interesting that the number of groups detected is practically the same as that for the initial sample: just their acidic strength increases, as a result of oxidation, which is related to the number of active sites on the PANI compound. The same is noticed for the PANI-C sample.

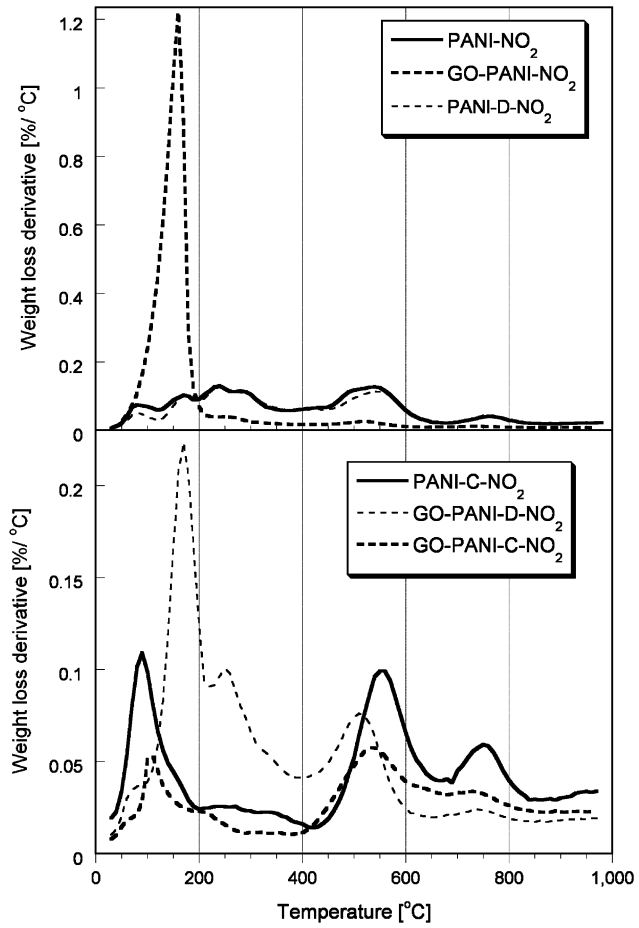


**Figure 10.** DTG after $NO_2$ adsorption.

The exposure to $NO_2$ practically does not change the XRD spectra (see Figure 8). On the other hand, the DTG curves after $NO_2$ reduction (Figure 10) show the changes in the chemical nature of the materials, by a decrease in the intensity of the peak at ~500 °C that is associated with the aromatization of the compound, accompanied by the removal of hydrogen. Oxidation of emeraldine with $NO_2$ decreases the amounts of decomposition gases released in the range of 400−600 °C. Moreover, for all samples that have been exposed to $NO_2$, the increase in intensity of the peak associated with the removal of water is noticeable, because $H_2O$ is a product of the surface reaction. The increased weight loss in the range of 200−400 °C that is clearly visible for the GO-PANI-C sample used for $NO_2$ reduction can be explained by a different decomposition pattern of oxidized emeraldine (pernigraniline), in comparison with its reduced form.

## Conclusions

The results presented in this paper show the predominant effect of emeraldine salts and its calcined (partially reduced) counterparts on the reduction of $NO_2$ on graphite oxide−polyaniline (GO-PANI) composites. Although the GO has a positive effect on $NO_2$/NO retention on the surface of the composite when *N*-methylformamide is used as a solvent, via its retention between layers (and thus causing an increase in the number of sites for polar interactions), generally, for dried and calcined samples, its surface is inactive for $NO_2$ reduction. This is caused by the decomposition of oxygen-containing groups that are engaged in the reactions with emeraldine, which results in the conversion of GO to graphite layers, where $NO_2$/NO are not able to be intercalated between layers. The high activity of emeraldine is linked to its susceptibility to oxidation with pernigraniline, with NO and water as the reaction products. It is important to mention that, although, in real life, conditions other gases such as $H_2S$ or CO can be present, PANI that has been doped in GO is not expected respond well to (or to interact with) those contaminants. Although $H_2S$ can interact with the oxidized quinoid form of the polymer, it should not attack the −N−H bond in the reduced benzoic structure.

## Acknowledgment

The work was supported by ARO (under Grant No. W911NF-05-1-0537). The authors are grateful to Dr. Volodymyr Tsyalkovskyy from Clemson University for fruitful discussion on the chemistry of polyaniline compounds. T.J.B. thanks Dr. Jacek Jagiello for supplying the SAIEUS software.

## Literature Cited

(1) Brodie, B. C. *Ann. Chim . Phys.* **1860**, *59*, 466.

(2) Szabo, T.; Tombacz, E.; Illes, E.; Dekany, I. Enhanced acidity and pH-dependent surface charge characterization of successively oxidized graphite oxides. *Carbon* **2006**, *44*, 537.

(3) Lerf, A.; He, H.; Forster, M.; Klinowski, J. Structure of graphite oxide revisited. *J. Phys. Chem B* **1998**, *102*, 4477.

(4) Szabo, T.; Berkesi, O.; Dekany, I. DRIFT study of deuterium-exchanged graphite oxide. *Carbon* **2005**, *43*, 3181.

(5) Buchsteiner, A.; Lerf, A.; Pieper, J. Water dynamics in graphite oxide investigated with neutron scattering. *J. Phys. Chem. B* **2006**, *110*, 22328.

(6) Ramesh, P.; Bhagyalakshmi, S.; Sampath, S. J. Preparation and physicochemical and electrochemical characterization of exfoliated graphite oxide. *Colloid Interface Sci.* **2004**, *274*, 95.

(7) Schniepp, H. C.; Li, J.-L.; McAllister, M. J.; Sai, H.; Herrera-Alonso, M.; Adamson, D. H.; Prud'homme, R. K.; Car, R.; Saville, D. A.; Askay, I. A. Functionalized single graphene sheets derived from splitting graphite oxide. *J. Phys. Chem. B* **2006**, *110*, 8535.

(8) Kovtyukhova, N. I.; Ollivier, P. J.; Martin, B. R.; Mallouk, T. E.; Chizhik, S. A.; Buzaneva, E. V.; Gorchinskiy, A. D. Layer-by-layer assembly of ultrathin composite films from micron-sied graphite oxide sheets and polycations. *Chem. Mater.* **1999**, *11*, 771.

(9) Cerezo, F. T.; Preston, C. M. L.; Shanks, R. A. Structural, mechanical and dielectric properties of poly(ethylene-co-methyl acrylate-co-acrylic acid) graphite oxide nanocomposites. *Comput. Sci. Technol.* **2007**, *67*, 79.

(10) Liu, Z-H.; Wang, Z-M.; Yang, X.; Ooi, K. Intercalation of organic ammonium ions into layered graphite oxide. *Langmuir* **2002**, *18*, 4926.

(11) Bourlinos, A. B.; Gournis, D.; Petridis, D.; Szabo, T.; Szeri, A.; Dekany, I. Graphite oxide:chemical reduction to graphite and surface modification with primary aliphatic amines and amino acids. *Langmuir* **2003**, *19*, 6050.

(12) Wang, G.; Yang, Z.; Li, X.; Li, Ch. Synthesis of poly(aniline-co-*o*-anisidine)-intercalated graphite oxide composite by delamination/reassembling method. *Carbon* **2005**, *43*, 2564.

(13) Bissessure, R.; Liu, P. K. Y.; White, W.; Scully, S. F. Encapsulation of polyanilines into graphite oxide. *Langmuir* **2006**, *22*, 1729.

(14) Nethravathi, C.; Rajamathi. M. Delamination, colloidal dispersion and reassembly of alkylamine intercalated graphite oxide in alcohols. *Carbon* **2006**, *44*, 2635.

(15) Hummers, W. S.; Offeman, R. E. Preparation of graphite oxide. *J. Am. Chem. Soc.* **1958**, *80*, 1339.

(16) Bagreev, A.; Bashkova, S.; Locke, D. C.; Bandosz,.T. J. Sewage sludge derived materials as efficient adsorbents for removal of hydrogen sulfide. *Environ. Sci. Technol.* **2001**, *35*, 1537.

(17) Dubinin, M. M. In *Chemistry and Physics of Carbon*; Walker, P. L., Ed.; Marcel Dekker: New York, 1966; Vol. 2, pp 51−120.

(18) Jagiello, J.; Bandosz, T. J.; Schwarz, J. A. Carbon surface characterization in terms of its acidity constant distribution. *Carbon* **1994**, *32*, 1026.

(19) Jagiello, J. Stable numerical solution of the adsorption integral equation using splines. *Langmuir* **1994**, *10*, 2778.

(20) Seredych, M.; Bandosz, T. J. Removal of ammonia by graphite oxide via its intercalation and reactive adsorption. *Carbon* **2007**, *45*, 2130−2132.

(21) Tsai, T.-C.; Tree, D. A.; High, M. S. Degradation Kinetics of Polyaniline Base and Sulfonated Polyaniline. *Ind. Eng. Chem. Res.* **1994**, *33*, 2600.

(22) Traore, M. K.; Stevenson, W. T. K.; McCormick, J.; Dorey, R. C.; Wen, S.; Mayers, D. Thermal Analysis of polyaniline, Part I. Thermal degradation of HCl-doped emeraldine base. *Synth. Met.* **1991**, *40*, 137.

(23) (a) Zawadzki, J. IR spectroscopy in carbon surface chemistry. In *Chemistry and Physics of Carbon*; Thrower, P. A., Ed.; Marcel Dekker: New York, 1989; pp 180−200. (b) *The Sadtler Handbook of Infrared Spectra*; Simons, W. W., Ed.; Sadtler Research Laboratories: Philadelphia, PA, 1978. (c) Trenter, G.; Holmes, J.; Lindon, J. *Encyclopedia of Spectroscopy and Spectrometry*; Academic Press: New York, 2000.

(24) Baibarac, M.; Baltog, I.; Lefrant, S.; Mevellec, J. Y.; Chauvet, O. Polyaniline and carbon nanotubes based composites containing whole units and fragments of nanotubes. *Chem. Mater.* **2003**, *15*, 4149.

(25) Elizalde-Torres, J.; Hu, H.; Saniger, J. M. Comparison of $NO_2$ and $NH_3$ gas adsorption on semiconductor polyaniline films. *Rev. Mex. Fis.* **2005**, *51*, 482.

(26) Bourdo, S. E.; Viswanathan, T. Graphite/polyaniline (GP) composites: synthesis and characterization. *Carbon* **2005**, *43*, 2983.

(27) Quillard, S.; Louarn, G.; Lefrant, S.; MacDiarmid, A. G. Vibrational analysis of polyaniline: A comparative study of leucoemeraldine, emeraldine and pernigraniline bases. *Phys. Rev. B* **1994**, *50*, 12496.

(28) Stejskal, J.; Trchova, M.; Prokes, J.; Sapurna, I. Brominated Polyaniline. *Chem. Mater.* **2001**, *13*, 4083.

(29) Liu, P.; Gong, K. Synthesis of polyaniline-intercalated graphite oxide by in situ oxidative polymerization reaction. *Carbon* **1999**, *37*, 701.

*Received for review* March 28, 2007
*Revised manuscript received* July 5, 2007
*Accepted* July 29, 2007

IE070458A